

# Beyond the Typical: Modeling Rare Plausible Patterns in Chemical Reactions by Leveraging Sequential Mixture-of-Experts

Taicheng Guo<sup>1</sup> ✉, Changsheng Ma<sup>2</sup>, Xiuying Chen<sup>2</sup>, Bozhao Nan<sup>1</sup>, Kehan Guo<sup>1</sup>  
Shichao Pei<sup>3</sup>, Nitesh V. Chawla<sup>1</sup>, Olaf Wiest<sup>1</sup>, Xiangliang Zhang<sup>1</sup> ✉✉

<sup>1</sup>University of Notre Dame, <sup>2</sup>King Abdullah University of Science and Technology,

<sup>3</sup>University of Massachusetts Boston

✉{tguo2, xzhang33}@nd.edu

## Abstract

Reaction prediction, a critical task in synthetic chemistry, is to predict the outcome of a reaction based on given reactants. Generative models like Transformer and VAE have typically been employed to predict the reaction product. However, these likelihood-maximization models overlooked the inherent stochastic nature of chemical reactions, such as the multiple ways electrons can be redistributed among atoms during the reaction process. In scenarios where similar reactants could follow different electron redistribution patterns, these models typically predict the most common outcomes, neglecting less frequent but potentially crucial reaction patterns. These overlooked patterns, though rare, can lead to innovative methods for designing synthetic routes and significantly advance synthesis techniques. To break the limits of previous approaches, we propose organizing the mapping space between reactants and electron redistribution patterns in a divide-and-conquer manner. We address the reaction problem by training multiple expert models, each specializing in capturing a type of electron redistribution pattern in reaction. These experts enhance the prediction process by considering both typical and other less common electron redistribution manners. In the inference stage, a *dropout* strategy is applied to each expert to improve the electron redistribution diversity. The most plausible products are finally predicted through a *ranking* stage designed to integrate the predictions from multiple experts. Experimental results on the largest reaction prediction benchmark USPTO-MIT show the superior performance of our proposed method compared to baselines.

## Introduction

Reaction outcome prediction is one of the fundamental problems in computer-assisted organic synthesis. The aim of this task is to predict the products formed given a set of reactants and reagents (Corey and Wipke 1969; Coley et al. 2017; Keto et al.). Prior solutions for this task can be grouped into two main categories: template-based (Segler and Waller 2017a,b) and template-free (Jin et al. 2017). Template-based methods are typically rule-based and rely heavily on expert knowledge for generalizing reaction patterns and mechanistic pathways. The knowledge requirement and the labor-intensive nature of template creation constrain these methods’ scalability and

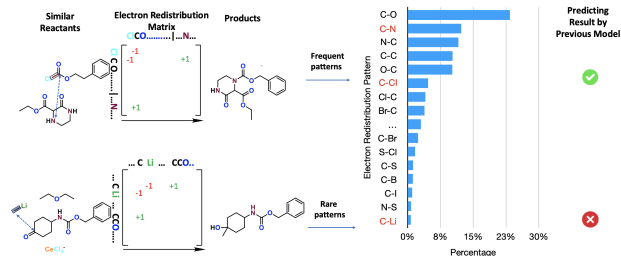


Figure 1: Examples of reactions with similar reactants, however, taking different electron flow patterns. ‘+1’ indicates forming a new bond, and ‘-1’ indicates breaking an existing bond. Current models are optimized to capture the most probable redistribution patterns. As a result, when presented with input reactants similar to the example, these models tend to associate them with frequent patterns (Carbon atoms tend to combine with nitrogen and chlorine atoms) while overlooking rare ones (Carbon atoms bond with silicon atoms).

adaptability, struggling with novel or unconventional reactions. To tackle these limitations, template-free methods leverage deep generative models to predict products from reactants. Indeed, while generative models such as Seq2Seq (Sutskever, Vinyals, and Le 2014; Guo et al. 2023b,c) or conditional VAE (Sohn, Lee, and Yan 2015; Ma et al. 2024) are powerful for predicting chemical reaction products, the training objective for these models is to maximize the likelihood based on a given training dataset. Generally, this objective is to fit models to the training dataset, where similar inputs typically are mapped to similar outputs. However, for reaction prediction tasks, similar inputs may produce entirely different outputs due to the stochastic nature and complex electron redistribution patterns during reaction. To better illustrate this problem, we show the Electron Redistribution Patterns (ERP) among atoms during the reaction process in Fig. 1. In chemical reactions, electrons are redistributed among the reacting molecules, either through transfer, sharing, or rearrangement, which directly influences the formation of new bonds and the breaking of existing ones. In common reactions like substitution or addition, electron redistribution patterns are consistent and well-represented in training datasets. However, rare patterns arise in complex or less typical reactions, such as those with competing pathways or extreme condi-

\*Corresponding author.

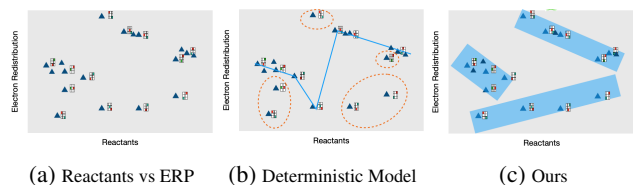


Figure 2: Reaction Prediction - mapping reactants to their corresponding Electron Redistribution Patterns (ERP).

tions. These rare patterns are harder to predict due to their infrequency in training data and the non-intuitive electron movements they often involve. **Note that two similar reactants can have entirely different electron redistribution patterns, with one being frequent and the other rare.** This challenges significantly complicate the task of accurately predicting reaction outcomes.

As illustrated in Fig. 2(a), identical or similar reactants (sharing similar x-axis coordinate values) could correspond with different ERP (varying y-axis coordinate values). A deterministic prediction which targets the maximum likelihood objective can only handle the most possible mapping between reactants and ERP and overlook the rare patterns (see Fig. 2(b), the overlooked redistribution are circled). An ideal reaction prediction model should 1) learn optimal mapping functions that capture both frequent and rare patterns, and 2) incorporate a degree of randomness to align with the inherent stochastic nature of chemical reactions. Drawing an analogy from chess move prediction, the model should be capable of predicting moves for both common and uncommon board states. Additionally, it should account for the inherent randomness in players’ strategies, influenced by factors such as ranking differences, emotional states, and individual characteristics. In our case, the variability can be caused by reaction conditions like temperature, solvent, and operator choices.

Drawing upon the inspirations of mixture-of-experts (MoE) models, we propose an approach utilizing a group of experts to learn multiple mapping functions corresponding to various electron flow patterns. One primary expert, with slight variations introduced by a dropout strategy, concentrates on the most common flow patterns. Meanwhile, other specialized experts, also with minor variations due to dropout, are dedicated to a range of diverse and rare patterns. To ensure that these experts can examine the entire training set from diverse perspectives of electron flow, we adopt a *divide-and-conquer* strategy, assigning experts different training samples based on distinct electron redistribution patterns. This approach emphasizes dividing and conquering according to electron redistribution patterns, rather than dividing reactants exclusively by their own features. Therefore, compared to a traditional MoE model, which directs similar reactants to the same expert using a gating function and typically results in only the most likely prediction, our MoE model can engage multiple experts for a single set of reactants. This approach leads to predictions that go beyond the typical, allowing the model to capture other rare but plausible electron flow patterns.

Since the electron redistribution matrix explicitly show-

cases the flow of electron redistribution, we creatively utilize the prediction loss of the electron redistribution matrix during training to autonomously partition the training samples among different experts. In particular, training samples with high loss are iteratively reassigned to new experts until all samples can be effectively managed. This sequentially trained MoE creates a team of experts each with a unique viewpoint regarding the electron redistribution flow within the entire input training set. Complemented by the application of *Dropout*, the *Sequential MoE* model can effectively explore a wider range of diverse electron flow patterns, as shown in Fig. 2(c). The underlying principle here is that dropout enables the creation of diverse neural networks by allowing a random subset of neurons to be nullified. Each distinct neural network conceived in this manner represents a spectrum of potentialities for electron flow within a smaller range. Comparing to previous methods, our approach has an array of model variations, enabling a comprehensive exploration of the reaction space. Last, at the inference stage, a simple ranking method is designed to prioritize most plausible products predicted by the model variations, maintaining an optimal balance between accuracy and diversity in predictions.

Our **main contributions** are summarized as follows:

- To the best of our knowledge, we are the first to investigate the issue of going beyond typical electron flow patterns in reaction prediction. This is a critical and specialized challenge presented to generative models when applying AI to scientific discovery.
- We innovatively resolve the identified challenges by designing a sequential MoE model with dropout to inclusively capture varied electron flow patterns, especially the rare ones, beyond the typical.
- Our method’s efficacy is validated through experiments on USPTO-MIT dataset (Jin et al. 2017), demonstrating consistent advancements and low latency over existing baselines.

## Related Work

**Reaction Prediction:** Machine learning methods for reaction prediction can be categorized as template-based and template-free. Template-based methods (Segler and Waller 2017a,b), although effective, rely heavily on expert knowledge and tend to be less generalizable. Among template-free methods, most solutions are autoregressive methods which either model reactions as a sequence of graph edits (Shi et al. 2020; Coley et al. 2017) or as a seq2seq translation (Liu et al. 2017; Schwaller et al. 2019; Guo et al. 2023a; Fang et al. 2024). To address the drawbacks of autoregressive generation, NERF (Bi et al. 2021) is proposed to model electron redistribution in a non-autoregressive way. ReactionSink (Meng et al. 2023) extends NERF by imposing two essential rules of electron redistribution during generation. Our MoE framework can be applied to any reaction prediction model. In this paper, we equip each expert by NERF, a state-of-the-art and open-sourced reaction prediction model, to demonstrate the effectiveness of our approach.

**Mixture-of-Experts:** In earlier years, MoE has been widely studied in the machine learning community (Jordan and

Jacobs 1994; Jacobs et al. 1991). The general methodology behind MoE is to train multiple experts and each specializes in a different part of the input (Chen et al. 2022). Then the outputs of different experts are aggregated to obtain the final output. However, the key challenge in reaction prediction is capturing the diverse electron flow patterns, which requires experts to specialize in capturing specific mappings to these patterns rather than being solely assigned to handle reactants based on their features. Therefore, we specially design a sequential training and gating method that enables different experts to effectively capture a wide range of electron flow patterns in reaction prediction.

**Dropout:** Dropout (Srivastava et al. 2014; Gal and Ghahramani 2016) is a common technique used to improve the generalization of neural networks. It operates by randomly omitting a unique subset of neurons during each training iteration, preventing the network from becoming overly sensitive to the specific weights of neurons. In our work, we deviate from the conventional motivation behind Dropout. We utilize the variability induced by selecting different neuron subsets through Dropout to model the small-range uncertainty present in the reaction prediction task. Thus, contrasting with conventional approaches that implement Dropout exclusively during training, we incorporate it during the inference phase. This approach facilitates the construction of slightly divergent models in each sampling process, allowing us to explore subtle differences in the predicted outcomes.

## The Proposed Solution

Following the definition of previous reaction prediction methods (Bi et al. 2021), we formulate the reaction prediction as a transformation from reactants  $G^r = (V^r, E^r)$  to products  $G^p = (V^p, E^p)$ .  $V^r$  and  $V^p$  denote the atoms, and  $E^r$  and  $E^p$  denote the number of shared electrons between atoms in the reactants and products, respectively. For example,  $E_{ij}$  denotes the number of shared electrons (1 denotes single bond and 2 denotes double bond) between atom  $i$  and atom  $j$ . The aim of the reaction prediction task is to learn a function  $f$  that can predict the potential product list  $P$  given the reactants  $G^r$ . The ground-truth product  $G^p$  should be at the top of the predicted product list  $P$ .

### Preliminary: The Architecture of A Single Expert for Reaction Prediction

We first introduce the Encoder-Decoder architecture of a single expert for reaction prediction. Given reactants  $G^r$ , an encoder is applied to transform reactants as representation vectors. The Encoder is implemented by Graph Neural Networks (GNN) (Scarselli et al. 2008; Fang et al. 2023) to capture the local dependency between atoms in  $G^r$ , followed by a Transformer (Vaswani et al. 2017) to model the long-range dependency between atoms. After encoding,  $G^r$  is represented by  $h^r$ ,

$$h^r = \text{Transformer}(\text{GNN}(G^r)). \quad (1)$$

Following the setting in NERF, PointerNet (Vinyals, Fortunato, and Jaitly 2015) is employed to compute the probabilities of an electron flow between atoms. Based on the Octet

Rule, the number of active valence electrons in an atom is generally at most 8. Therefore, 16 independent PointerNets are used to compute the attention weights between atoms to represent the *BondFormation*  $w_{ij}^{(+d)}$  and *BondBreaking*  $w_{ij}^{(-d)}$ , where  $w_{ij}$  denotes the attention weights (i.e. probability of an electron flow from  $i$  to  $j$ ), and  $d = 1, 2, \dots, 8$ . The values  $w_{ij}^{(+d)}, w_{ij}^{(-d)}$  are all between 0 and 1,

$$\begin{aligned} w_{ij}^{(+d)} &= \text{PointerNet}_d^+(h^r, i, j), d \in 1, 2, \dots, 8 \\ w_{ij}^{(-d)} &= \text{PointerNet}_d^-(h^r, i, j), d \in 1, 2, \dots, 8 \end{aligned} \quad (2)$$

Based on the electron flow probability  $w_{ij}^{(+d)}$  and  $w_{ij}^{(-d)}$ , the overall bond changes between reactants and products denoted by  $\Delta w_{ij}$  can be calculated by:

$$\Delta w_{ij} = \sum_{d=1}^8 w_{ij}^{(+d)} - \sum_{d=1}^8 w_{ij}^{(-d)}. \quad (3)$$

Adding  $\Delta w_{ij}$  to the reactant edges  $E^r$ , we can obtain the predicted product edges  $\hat{E}^p$ . The overall prediction loss is defined as the squared error between the ground-truth products and the predicted products:

$$L = \sum_{(i,j) \in E^p} \left( E_{ij}^p - \hat{E}_{ij}^p \right)^2. \quad (4)$$

### Sequential Training of Mixture-of-Experts

To learn the mapping functions for various electron flow patterns, we sequentially train a group of experts, as shown in Fig. 3. Besides the chief expert model, the entire trained model also includes  $F = \{(f_1, s_1), (f_2, s_2), \dots, (f_n, s_n)\}$ , where each expert  $f_i$  is associated with a set of training samples that the expert handled correctly. The  $s_i$  sets will be used during the inference stage for expert routing, guiding the selection of most appropriate expert(s) for making prediction.

To specialize each expert in learning specific mapping functions from input to output, we adopt a divide-and-conquer strategy that assigns different experts to distinct training samples based on varying electron redistribution patterns. Since the electron redistribution matrix is directly involved in the loss calculation (Eq. (4)), the loss function inherently evaluates how well each expert handles specific electron redistribution patterns. Thus, during training, we utilize the prediction loss of the electron redistribution matrix to autonomously partition the training samples among the experts. Concretely, after a warm-up phase, we train the first expert  $f_1$  and identify  $s_1$  as the set of training samples that  $f_1$  predicts correctly, defined as  $s_1 = \{(G^r, G^p) \in D_1 \mid L(f_1(G^r), G^p) = 0\}$ . The training dataset  $D_1$  is then updated by excluding  $s_1$ , resulting in  $D_2 = D_1 - s_1$ . The second expert  $f_2$  is trained by continuing the tuning of  $f_1$  on the updated dataset  $D_2$ . Similarly  $s_2$  is defined as  $s_2 = \{(G^r, G^p) \in D_2 \mid L(f_2(G^r), G^p) = 0\}$ . The third expert  $f_3$  is then obtained by further tuning  $f_2$  on the next updated dataset  $D_3 = D_2 - s_2$ . The whole process continues until the dataset is fully partitioned or a specified number of experts has been trained.

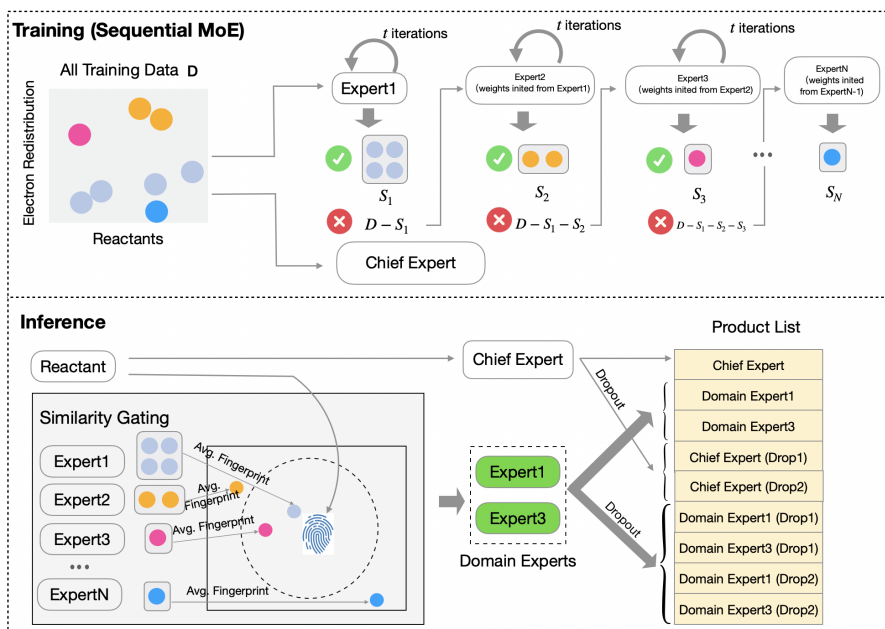


Figure 3: The overall framework of our proposed solution.

The detailed steps in this procedure are justified as follows:

**1) Warm-Up Phase:** The warm-up phase initializes one expert (the architecture of a single expert introduced previously) by training it for several iterations using the entire training dataset. This step is crucial to ensure that the expert, when engaged in sequential training, is proficient in recognizing basic reactions. **2) Training of Each Expert:** Each expert  $f_i$  is trained over  $t$  iterations. The samples in  $s_i$  are identified as those consistently predicted correctly across all  $t$  iterations, rather than basing our judgment on a single iteration. This approach ensures that the expert has reliably learned the patterns associated with those samples and the set  $s_i$  will effectively guide expert selection during the inference stage.

Moreover, we train a Chief Expert,  $f_{chief}$ , by utilizing the entire data until convergence, aiming to fully encapsulate the most common electron redistribution patterns. While it excels in generalization due to its comprehensive learning scope,  $f_{chief}$  tends to overlook rare electron redistribution patterns that are not well-represented in the overall dataset. Since the experts in  $F$  are specialized in capturing specific and rare electron redistribution patterns,  $f_{chief}$  serves as a complementary entity to these experts, enhancing the model’s ability to generalize across the entire reaction space while ensuring common patterns are robustly covered.

### Inference Stage of Reaction Prediction

**Expert Selection.** Unlike the original MoE method, which uses the same gating network for routing the input during both training and inference, our model organizes the training of experts by dividing samples based on their electron redistribution patterns. During inference, the testing input is directed to multiple experts based on its fingerprint features. Specifically, each testing sample is compared with the sets  $s_i$  to identify multiple experts  $f_i$  that exhibit high similarity with the input, as illustrated in Fig. 3. Concretely, we

compute the average of the Morgan Fingerprint (Capecchi, Probst, and Reymond 2020) (radius=2) of the reactants in  $s_i$  to derive the Expert Fingerprint for each expert  $f_i$ . For each test reactant  $G^r$ , we compute the cosine similarity between its Morgan Fingerprint and the Expert Fingerprint of each expert  $f_i$  in  $F$ . Subsequently, the Top- $N$  most analogous experts to the test reactants are selected, denoted as  $TopN$ , and ranked in descending order based on Fingerprint similarity for the subsequent prediction phase. We use Fingerprint similarity because it effectively captures the structural similarities between molecules and offers a complementary perspective that GNN-learned representations may not capture, enabling more accurate matching between the test reactants and the specialized experts.

**Inference-time Dropout.** By applying dropout at test time and running multiple forward passes with different dropout masks, a predictive model generates a distribution of predictions, offering insights into its uncertainty in prediction. This technique, known as Monte Carlo Dropout (Gal and Ghahramani 2016), aligns well with our objective of capturing the inherent stochastic nature of chemical reactions in our prediction model. During the inference stage, we apply dropout to both the GNN encoder and the self-attention layer of the Transformer encoder for each selected expert  $f_i$ . Since the dropout layers are influenced by the random seed, we vary the seed for each inference iteration to introduce variability in the predictions. This process is repeated five times to generate a list of predicted products for each model. To obtain models with minor variations while retaining general chemical reaction patterns, a low dropout rate (0.1) is applied in our experiments.

**Ranking for the Final Prediction.** Unlike the conventional MoE which applies a weighted sum to the outputs of each expert to get one single predicted value, our model generates

a number of products that need to be ranked to move the most likely product to the front of the list. We first collect the predictions produced by four types of experts: the chief expert ( $f_{chief}$ ), the chief expert with dropout ( $f_{chief}^{drop}$ ), the selected experts ( $f_s$ ), and selected experts with dropout ( $f_s^{drop}$ ). Each expert model in  $f_{chief}$  and  $f_s$  is run once, while each of  $f_{chief}^{drop}$  and  $f_s^{drop}$  is run five times with different random seeds for producing the predictions. By evaluating the performance of these four types of experts on a validation set (results shown in Table 4 and 3), we designed an empirically effective ranking method to order all the predicted products. Since  $f_{chief}$  achieves the best Top-1 Accuracy, we place its predictions at the top of the predicted product list, followed by the predictions from  $f_s$ ,  $f_{chief}^{drop}$ , and  $f_s^{drop}$ , as shown in the bottom part of Fig. 3. Regarding the predictions made by the selected experts  $f_i$  in  $f_s$  and  $f_s^{drop}$ , they are ranked according to the Fingerprint similarity to the test reactants in  $TopN$  associated with them, as explained earlier in ‘Expert Selection’ section. For the rank of predictions made by the same expert using different random seeds, we simply order the predictions sequentially based on the random seed values used.

## Experiments

### Experiment Settings

**Datasets and preprocessing.** Same as most previous work (Coley et al. 2019; Schwaller et al. 2019), we evaluate our method on the current largest public reaction prediction dataset USPTO-MIT (Jin et al. 2017). There are 479K reactions in this dataset and the default train-test splits are widely adopted in all baselines and our method. To assess our model’s performance in capturing the “rare” electron redistribution patterns, we specifically select reactions where the electron flow percentage is less than 1% and test our model on these reactions. Following the preprocessing step in NERF (Bi et al. 2021), 0.3% of USPTO-MIT reactions do not satisfy the non-autoregressive learning settings. Thus we also remove such reactions from both training and testing and subtract the predictive Top-k accuracy by 0.3% as the final accuracy of our model.

**Implementation details.** We implement our model using Pytorch (Paszke et al. 2019) and conduct all the experiments on a Linux server with GPUs (4 Nvidia V100). As mentioned in Section 3.2, we reuse the encoder and decoder architectures from the NERF model. To ensure a fair comparison to previous non-autoregressive methods, we follow the same detailed settings as the previous model. We set the number of self-attention layers in the Transformer encoder and decoder to 6, and the number of attention heads is 8. We also set the node embedding dimension to 256 and use the AdamW optimizer (Loshchilov and Hutter 2017) at a learning rate  $10^{-4}$  with linear warmup and learning rate decay. For the sequential training, we set the maximum sequential training iteration to 80 and the update interval for each expert  $t$  to 2. For the similarity gating, the set of  $N$  depends on the Top-K evaluation metrics. Since the maximum K in our evaluation is 10, we set  $N$  to 2 and it’s enough to have sufficient candidates.

So for each test reactants, we only use three experts (Chief experts and two specialized experts) to predict the products. The implementation code will be made publicly available upon the acceptance of the paper.

**Evaluation metrics.** Following (Coley et al. 2019; Schwaller et al. 2019; Bi et al. 2021; Meng et al. 2023), we use the Top-K accuracy to evaluate the performance of our model and baselines. The Top-K accuracy measures the percentage of reactions that have the ground-truth product in the Top-K predicted products. Following the previous setting, the  $K$  is set as: {1, 2, 3, 5, 10}. For test reactants that have more than two products in the USPTO-MIT dataset, we assess prediction performance by calculating the reactant-wise HitRate@K, which is the percentage of products appearing in the K predicted products that are also in the ground truth. It also means how many of the multiple ground truth products are correctly identified by the model among its predictions.

### Baselines

We compare our method with the following baselines which are classified into four categories:

**Template-based.** Symbolic (Qian et al. 2020) introduces symbolic inference which is based on chemical rules to the neural network to do reaction prediction.

**Autoregressive.** MT-based (Schwaller et al. 2019), Chemformer (Irwin et al. 2022), Graph2Smiles (Tu and Coley 2022) are various models for reaction prediction. MT-based treats the problem as SMILES string translation using transformers. Chemformer is also a transformer-based model and uses a pretrained SMILES encoder with self-supervised tasks. Graph2Smiles combines graph encoding with transformer decoding to achieve permutation-invariance encoding of molecule graphs.

**Non-autoregressive.** NERF (Bi et al. 2021) is the first and widely used to model reaction prediction in a non-autoregressive way; ReactionSink (Meng et al. 2023) is based on NERF and integrates two essential chemical rules of electron redistribution to NERF via Sinkhorn’s algorithm. Both of them are based on the CVAE architecture and leverage the latent variable of a prior to introduce randomness. Our method can be applied to both of them. However, due to the lack of open-source code and the instability of ReactionSink, we haven’t tested our method with it. We test our method with NERF which is more widely used and stable. Additional test will be conducted once the code of ReactionSink is released.

### Reaction Prediction Performance

The performance of evaluated models for rare reaction patterns and overall performance measured by Top-K accuracy is reported in Table 1. **1) Improvements on prediction with rare reaction patterns.** We can see that our method improves the NERF model, resulting in the highest Top-1 to Top-10 accuracy. In our ranking list, the chief expert is ranked first, followed by two specialized experts. As shown in Table 1, the top-2 and top-3 accuracy demonstrate more significant improvement compared to the top-1 accuracy. This improvement can be attributed to the effectiveness of the two specialized experts. The predictions made by the experts with

Table 1: The Top-K Accuracy % and Latency of evaluated models in the USPTO-MIT dataset, top: performance on rare reaction patterns; bottom: overall performance on all reactions. The best results are in bold font. †: results from corresponding papers.

Category	Model	Accuracy on rare reaction patterns						Latency (ms)
		Top-1	Top-2	Top-3	Top-5	Top-10	Avg.	
Template-based	Symbolic	85.1	88.9	90.5	92.0	92.8	89.9	1130
Autoregressive	MT-base	85.9	90.5	91.7	92.4	92.7	90.6	227
	Chemformer	88.3	90.6	91.0	91.4	91.7	90.6	1714
	Graph2Smiles	88.2	91.7	92.7	93.5	94.3	92.1	633
Non-autoregressive	NERF	89.2	90.4	90.9	91.1	91.1	90.5	20.6
	NERF+Our method	<b>89.9 ± 0.0</b>	<b>92.1 ± 0.0</b>	<b>93.1 ± 0.06</b>	<b>94.0 ± 0.06</b>	<b>94.9 ± 0.1</b>	<b>92.8</b>	<b>20.2</b>

Category	Model	Accuracy on all test set					Parallel	Latency (ms)
		Top-1	Top-2	Top-3	Top-5	Avg.		
Template-based	Symbolic†	87.9	91.1	92.4	93.5	91.2	✓	1130
Autoregressive	MT-base†	88.8	92.6	93.7	94.4	92.4	×	227
	Chemformer†	90.9	93.1	93.5	93.8	92.8	×	1714
	Graph2Smiles†	90.3	93.1	94.0	94.6	93.0	×	633
Non-autoregressive	NERF	90.7±0.03	92.3±0.22	93.3 ± 0.15	93.7 ± 0.17	92.5	✓	20.6
	NERF+Our method	<b>91.5±0.00</b>	<b>93.5±0.06</b>	<b>94.3±0.00</b>	<b>95.0±0.06</b>	<b>93.6</b>	✓	<b>20.2</b>

dropout are ranked after the third place. The improvement in top-5 and top-10 accuracy verifies the effectiveness of incorporating dropout for capturing additional variability in the predictions. **2) Overall performance.** Our method also behaves the best on all test set, while achieving lower latency. Overall, the results in Table 1 indicate our method can capture multiple electron redistribution patterns beyond the typical.

### Ablation Studies

To further investigate the effect of each component of our method, we conduct ablation studies. The results are shown in Table 2. We created variant models by applying only the Sequential MoE training on top of NERF and by using only the Dropout strategies. Our observations show that using either design alone improves performance compared to the original NERF model. The performance of the combination of these two strategies is the best. This demonstrates that each strategy is beneficial to the model and they can compensate each other and help achieve better performance.

Table 2: The impact of Seq.MoE, and Dropout, and their combination.

Model Name	Top-1	Top-2	Top-3	Top-5
NERF	90.7	92.3	93.3	93.7
NERF + Seq.MoE	<b>91.5</b>	93.3	93.7	94.0
NERF + Dropout	<b>91.5</b>	93.1	93.7	94.1
NERF + Seq.MoE + Dropout	<b>91.5</b>	<b>93.5</b>	<b>94.3</b>	<b>95.0</b>

### Performance of Different Ranking Methods

As discussed in ‘‘Ranking for the Final Prediction’’ section, to investigate which ranking strategy can achieve better performance, we evaluate all strategies on the validation set in Table 3. We can see that the order for the best accuracy is:  $f_{chief}, f_s, f_{chief}^{drop}$ , and  $f_s^{drop}$ , while the performance of these ranking strategies is highly similar.

To make further investigation, we test the performance of different experts in Table 4. Since the chief expert  $f_{chief}$  only makes one prediction, its Avg.L is 1. When applying dropout, the chief expert  $f_{chief}^{drop}$  can generate more than one distinct product. The specialized expert set  $f_s$ , which includes two

experts (TopN with N=2), often generates different products, resulting in an Avg.L of 2. Notably,  $f_s^{drop}$  has a large Avg.L=8.4 with Top-10 accuracy of 95.0, indicating that  $f_s^{drop}$  can generate diverse and accurate products. This clarifies that the similar performance of the ranking strategies is due to the small Avg.L of  $f_{chief}^{drop}$  and  $f_s$ .

Table 3: The performance of different ranking strategies on the validation set. From the left to right is the order placed in the product list.

Ranking strategies	Top-1	Top-2	Top-3	Top-5	Top-10
$f_{chief}, f_{chief}^{drop}, f_s, f_s^{drop}$	91.3	93.1	94.1	94.8	95.4
$f_{chief}, f_{chief}^{drop}, f_s^{drop}, f_s$	91.3	93.1	94.0	94.8	95.4
$f_{chief}, f_s, f_{chief}^{drop}, f_s^{drop}$	<b>91.3</b>	<b>93.4</b>	<b>94.2</b>	<b>94.9</b>	<b>95.4</b>
$f_{chief}, f_s, f_s^{drop}, f_{chief}^{drop}$	91.3	93.2	94.0	94.7	95.3
$f_{chief}, f_s^{drop}, f_{chief}^{drop}, f_s$	91.3	93.2	94.0	94.7	95.3
$f_{chief}, f_s^{drop}, f_s, f_{chief}^{drop}$	91.3	93.2	94.0	94.7	95.3

Table 4: The performance of different kinds of experts on the validation set. The Avg.L represents the average number of distinct products in the predicted lists for each reaction in the test set. The unavailable case is indicated by -.

Experts	Top-1	Top-2	Top-3	Top-5	Top-10	Avg.L↑
$f_{chief}$	91.3	-	-	-	-	1.0
$f_{chief}^{drop}$	90.3	92.6	93.1	93.4	93.4	1.6
$f_s$	89.3	91.9	92.6	93.0	93.1	1.9
$f_s^{drop}$	87.9	91.7	93.1	94.2	95.0	8.4

### Latency and Sampling Efficiency

We examine the computational costs of our methods compared to the NERF model, specifically focusing on inference latency. Latency here refers to the time required to process a single test sample in one sampling iteration. As shown in Table 5, the latency of our model is almost the same as the NERF model. This is because compared to NERF model, removing the independent prior sampling reduces the latency by 1ms, and incorporating the similarity gating adds a mere 0.6ms.

Table 5: The Latency and Sampling Time (per sample) in ms, and corresponding performance of our methods and NERF.

Model Name	Latency	Time	Top-1	Top-2	Top-3	Top-5	Top-10
NERF	20.6	10	90.7	92.3	93.3	93.7	94.0
Ours	20.2	11	91.5	93.3	94.0	94.5	94.8
Ours (more samples)	20.2	21	91.5	93.3	94.1	94.7	95.0
Ours (even more)	20.2	31	91.5	93.3	94.1	94.8	95.2

We also compare the performance within different sampling time between our methods and NERF model. We adjust the dropout times for each expert to control the sampling time. NERF relies on sampling a prior latent vector from a Gaussian Distribution with the increasing variance. Our findings highlight two key points: **1)** The performance of NERF doesn’t scale with increased sampling, as higher variance leads to more invalid products. Specifically, the percentage of the valid predicted products generated by NERF model falls to 79.8%, 46.5%, and 8.6% at the 11th, 12th and 13th samplings, respectively. **2)** Our methods not only achieve superior results with just 11 samplings compared to NERF but also consistently produce more valid potential products.

### Insights for Scaling compared to Vanilla MoE

Our work also shows some inspiring model scaling insights for chemical reaction prediction and also for other scientific areas that emphasize on modeling rare patterns, instead of maximizing likelihood. As shown in Table 6, our method outperforms Vanilla MoE. Both our method and Vanilla MoE are designed for scaling up the model, traditional MoE designed for multi-task scenarios is limited in routing similar inputs to the same experts, failing to capture diverse transformation patterns from input to output and overlooking some patterns. Our Sequential-MoE can be regarded as routing similar transformation patterns to the same experts, thus improving the performance specifically for top-3 and top-10 accuracy.

Table 6: Our method vs the Vanilla MoE

Model Name	Top-1	Top-3	Top-10
NERF+Vanilla MoE	<b>91.7</b>	93.2	93.5
NERF+Our Method	91.5	<b>94.3</b>	<b>95.6</b>

### Evaluation on Multi-selectivity Reactions

Since it is difficult to accurately extract the reactions which contain overlooked electron transfer patterns to evaluate our methods, we conduct evaluations on multi-selectivity reactions, which are more likely to be influenced by the overlooked electron transfer patterns issue because the reactants are the same and their electron transfer are different. To simplify, we select the reactants that have more than two products in the USPTO-MIT dataset and compute the reactant-wise HitRate. Note that a higher HitRate would indicate that a higher percentage of the actual (ground truth) products are being correctly predicted. As shown in Table 7, we can see that our method has a higher HitRate than the NERF model, confirming that our method has enhanced capability for predicting multi-selectivity reactions.

Table 7: The HitRate of our method and NERF model in multi-selectivity reactions.

Model Name	HitRate@2	HitRate@3	HitRate@5	HitRate@10
NERF	0.305	0.312	0.315	0.315
NERF+Our Method	<b>0.315</b>	<b>0.338</b>	<b>0.348</b>	<b>0.358</b>

### Insights: Do we really need generative models for the Reaction Prediction Task?

All previous reaction prediction methods such as Chemformer (Irwin et al. 2022), Graph2Smiles (Tu and Coley 2022), and NERF (Bi et al. 2021) are generative models. Chemformer and Graph2Smiles use beam search with random sampling to generate diverse products. NERF builds on Conditional Variational Autoencoder, introducing a noise vector to sample diverse products. Our approach differs fundamentally from these, employing deterministic models with different variants for reaction prediction. The variants are created by building a set of specialized models and the application of MC dropout.

Our experiments, which demonstrate the superior performance of our proposed methods, prompt a reconsideration of the reaction prediction task. Given reactants, this task requires generating a limited set of diverse yet constrained products. While it shares similarities with generative model settings in producing varied outputs, it differs in three key aspects: (1) The number of generated products should be limited, not excessive. (2) Rare patterns are particularly important and should be accounted for. (3) Each generated product must strictly adhere to chemical reaction patterns.

Our work explores the potential to solve the reaction prediction task without using generative models. We hope our approach will inspire a reconsideration of the reaction prediction task and stimulate further research in this direction.

### Broader Impacts and Limitations

The most potentially positive impact is that our work is the first to identify the importance of the rare reaction redistribution patterns in reaction prediction and propose a significant method to solve it. Previous related methods focus on the overall performance and the model is prone to predict common patterns which are less helpful for reaction discovery. Our work has the potential to benefit other science domains that emphasize the discovery of “rare” patterns such as biology, materials, etc. However, the limitation of our work is that current experiments are only conducted in chemical reaction prediction. We will extend the application of this framework to other topics to continue the exploration of discovering rare patterns beyond typical.

### Conclusion

Reaction prediction is a fundamental and challenging task. In this paper, we identify the issue of overlooked electron redistribution patterns by all previous methods. To tackle this challenge, we design a framework that applies Sequential MoE and Dropout to support predictions that go beyond the typical, allowing the model to capture other rare but plausible electron flow pattern. Sequential MoE models capture the

large-range rare patterns while dropout can obtain small-difference models to capture the small-range rare patterns. We also designed a ranking method to order the predicted products of MoE to ensure the predicted products are as precise as possible. Experiment results show our model can consistently outperform the baselines.

## References

- Bi, H.; Wang, H.; Shi, C.; Coley, C.; Tang, J.; and Guo, H. 2021. Non-autoregressive electron redistribution modeling for reaction prediction. In *International Conference on Machine Learning*, 904–913. PMLR.
- Capecchi, A.; Probst, D.; and Reymond, J.-L. 2020. One molecular fingerprint to rule them all: drugs, biomolecules, and the metabolome. *Journal of cheminformatics*, 12(1): 1–15.
- Chen, Z.; Deng, Y.; Wu, Y.; Gu, Q.; and Li, Y. 2022. Towards understanding mixture of experts in deep learning. *arXiv preprint arXiv:2208.02813*.
- Coley, C. W.; Barzilay, R.; Jaakkola, T. S.; Green, W. H.; and Jensen, K. F. 2017. Prediction of organic reaction outcomes using machine learning. *ACS central science*, 3(5): 434–443.
- Coley, C. W.; Jin, W.; Rogers, L.; Jamison, T. F.; Jaakkola, T. S.; Green, W. H.; Barzilay, R.; and Jensen, K. F. 2019. A graph-convolutional neural network model for the prediction of chemical reactivity. *Chemical science*, 10(2): 370–377.
- Corey, E. J.; and Wipke, W. T. 1969. Computer-Assisted Design of Complex Organic Syntheses: Pathways for molecular synthesis can be devised with a computer and equipment for graphical communication. *Science*, 166(3902): 178–192.
- Fang, J.; Wang, X.; Zhang, A.; Liu, Z.; He, X.; and Chua, T.-S. 2023. Cooperative explanations of graph neural networks. In *Proceedings of the Sixteenth ACM International Conference on Web Search and Data Mining*, 616–624.
- Fang, J.; Zhang, S.; Wu, C.; Yang, Z.; Liu, Z.; Li, S.; Wang, K.; Du, W.; and Wang, X. 2024. Moltc: Towards molecular relational modeling in language models. *arXiv preprint arXiv:2402.03781*.
- Gal, Y.; and Ghahramani, Z. 2016. Dropout as a bayesian approximation: Representing model uncertainty in deep learning. In *international conference on machine learning*, 1050–1059. PMLR.
- Guo, T.; Guo, K.; Liang, Z.; Guo, Z.; Chawla, N. V.; Wiest, O.; Zhang, X.; et al. 2023a. What indeed can GPT models do in chemistry? A comprehensive benchmark on eight tasks. *arXiv preprint arXiv:2305.18365*.
- Guo, T.; Nan, B.; Liang, Z.; Guo, Z.; Chawla, N.; Wiest, O.; Zhang, X.; et al. 2023b. What can large language models do in chemistry? a comprehensive benchmark on eight tasks. *Advances in Neural Information Processing Systems*, 36: 59662–59688.
- Guo, T.; Yu, L.; Shihada, B.; and Zhang, X. 2023c. Few-shot news recommendation via cross-lingual transfer. In *Proceedings of the ACM Web Conference 2023*, 1130–1140.
- Irwin, R.; Dimitriadis, S.; He, J.; and Bjerrum, E. J. 2022. Chemformer: a pre-trained transformer for computational chemistry. *Machine Learning: Science and Technology*, 3(1): 015022.
- Jacobs, R. A.; Jordan, M. I.; Nowlan, S. J.; and Hinton, G. E. 1991. Adaptive mixtures of local experts. *Neural computation*, 3(1): 79–87.
- Jin, W.; Coley, C.; Barzilay, R.; and Jaakkola, T. 2017. Predicting organic reaction outcomes with weisfeiler-lehman network. *Advances in neural information processing systems*, 30.
- Jordan, M. I.; and Jacobs, R. A. 1994. Hierarchical mixtures of experts and the EM algorithm. *Neural computation*, 6(2): 181–214.
- Keto, A.; Guo, T.; Underdue, M.; Stuyver, T.; Coley, C. W.; Zhang, X.; Krenske, E. H.; and Wiest, O. Data-Efficient, Chemistry-Aware Machine Learning Predictions of Diels–Alder Reaction Outcomes. *Journal of the American Chemical Society*.
- Liu, B.; Ramsundar, B.; Kawthekar, P.; Shi, J.; Gomes, J.; Luu Nguyen, Q.; Ho, S.; Sloane, J.; Wender, P.; and Pande, V. 2017. Retrosynthetic reaction prediction using neural sequence-to-sequence models. *ACS central science*, 3(10): 1103–1113.
- Loshchilov, I.; and Hutter, F. 2017. Decoupled weight decay regularization. *arXiv preprint arXiv:1711.05101*.
- Ma, C.; Guo, T.; Yang, Q.; Chen, X.; Gao, X.; Liang, S.; Chawla, N.; and Zhang, X. 2024. A Property-Guided Diffusion Model For Generating Molecular Graphs. In *ICASSP 2024-2024 IEEE International Conference on Acoustics, Speech and Signal Processing (ICASSP)*, 2365–2369. IEEE.
- Meng, Z.; Zhao, P.; Yu, Y.; and King, I. 2023. Doubly Stochastic Graph-based Non-autoregressive Reaction Prediction. *arXiv preprint arXiv:2306.06119*.
- Paszke, A.; Gross, S.; Massa, F.; Lerer, A.; Bradbury, J.; Chanan, G.; Killeen, T.; Lin, Z.; Gimelshein, N.; Antiga, L.; et al. 2019. Pytorch: An imperative style, high-performance deep learning library. *Advances in neural information processing systems*, 32.
- Qian, W.; Russell, N.; Simons, C.; Luo, Y.; Burke, M.; and Peng, J. 2020. Integrating Deep Neural Networks and Symbolic Inference for Organic Reactivity Prediction. *10.26434/chemrxiv.11659563*.
- Scarselli, F.; Gori, M.; Tsoi, A. C.; Hagenbuchner, M.; and Monfardini, G. 2008. The graph neural network model. *IEEE transactions on neural networks*, 20(1): 61–80.
- Schwaller, P.; Laino, T.; Gaudin, T.; Bolgar, P.; Hunter, C. A.; Bekas, C.; and Lee, A. A. 2019. Molecular transformer: a model for uncertainty-calibrated chemical reaction prediction. *ACS central science*, 5(9): 1572–1583.
- Segler, M. H.; and Waller, M. P. 2017a. Modelling chemical reasoning to predict and invent reactions. *Chemistry–A European Journal*, 23(25): 6118–6128.
- Segler, M. H.; and Waller, M. P. 2017b. Neural-symbolic machine learning for retrosynthesis and reaction prediction. *Chemistry–A European Journal*, 23(25): 5966–5971.
- Shi, C.; Xu, M.; Guo, H.; Zhang, M.; and Tang, J. 2020. A graph to graphs framework for retrosynthesis prediction. In



International conference on machine learning, 8818–8827. PMLR.

Sohn, K.; Lee, H.; and Yan, X. 2015. Learning Structured Output Representation using Deep Conditional Generative Models. In Cortes, C.; Lawrence, N.; Lee, D.; Sugiyama, M.; and Garnett, R., eds., *Advances in Neural Information Processing Systems*, volume 28. Curran Associates, Inc.

Srivastava, N.; Hinton, G.; Krizhevsky, A.; Sutskever, I.; and Salakhutdinov, R. 2014. Dropout: a simple way to prevent neural networks from overfitting. *The journal of machine learning research*, 15(1): 1929–1958.

Sutskever, I.; Vinyals, O.; and Le, Q. V. 2014. Sequence to sequence learning with neural networks. *Advances in neural information processing systems*, 27.

Tu, Z.; and Coley, C. W. 2022. Permutation invariant graph-to-sequence model for template-free retrosynthesis and reaction prediction. *Journal of chemical information and modeling*, 62(15): 3503–3513.

Vaswani, A.; Shazeer, N.; Parmar, N.; Uszkoreit, J.; Jones, L.; Gomez, A. N.; Kaiser, L. u.; and Polosukhin, I. 2017. Attention is All you Need. In *Advances in Neural Information Processing Systems*, volume 30.

Vinyals, O.; Fortunato, M.; and Jaitly, N. 2015. Pointer networks. *Advances in neural information processing systems*, 28.

## Appendix

### Performance in Group-wise Prediction

We also investigate whether our method can help generate a more precise set of plausible products compared to NERF. For the test set, we group the reactions by the number of predicted products and compute the percentage and HitRate (how many ground-truth products are identified in the predicted products) for each group. Fig. 4(a) shows that our method predicts more accurate plausible products compared to NERF, aligning more closely with the real-world scenario where the quantity of plausible products adheres to a power-law distribution. The HitRate of our method for each group (in Fig. 4(b)) is higher than that of the NERF model, indicating our method can generate more precise products.

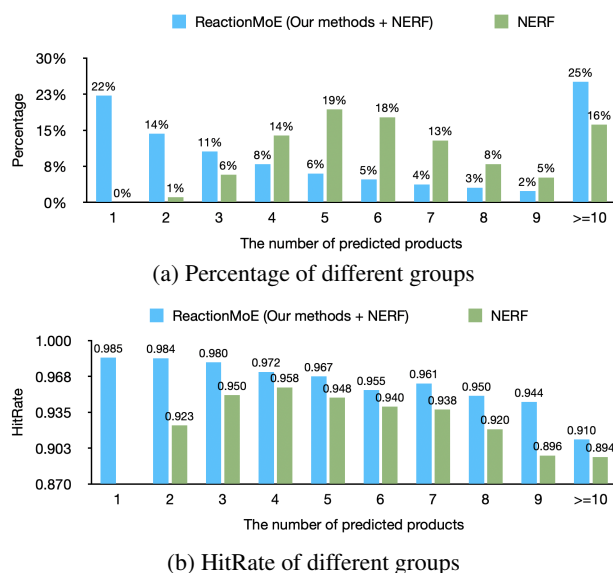


Figure 4: The Percentage and HitRate of test reactions grouped by the number of predicted products.

### The Training Procedure of Our Methods

The training procedure of our sequential mixture of experts is outlined in Algorithm 1. In our experiments, the training iterations for the warm-start is set to 20. The number of experts  $n$  is set to 40, and the training iterations for each expert  $t$  is set to 2. Hence, the training iterations for all experts exclude chief expert is 100. The training iterations for chief expert is 100 which is the same as the baseline (NERF). As the training dataset is progressively reduced during the process, the overall training time of our methods is less than twice the original training time.

### Implementation Details

We utilize the USPTO-MIT dataset<sup>1</sup>, which is the largest and most widely used dataset for reaction prediction research. Our code is included with this submission. Further implementation details are provided in the paper. We will release

<sup>1</sup><https://github.com/wengong-jin/nips17-rexgen/blob/master/USPTO/data.zip>

---

**Algorithm 1: Training Procedure of Sequential MoE**

---

**Require:** Training dataset  $D$ , the number of experts  $n$ , the training iteration for each expert  $t$

**Ensure:** A Dictionary which saves the pair of expert and the corresponding “correctness” training samples for this expert  $F = \{(f_1, s_1), (f_2, s_2), \dots, (f_n, s_n)\}$

- 1: Warm-start: Train initial model  $f$  on  $D$  for several iterations
- 2: Initialize  $D_i \leftarrow D$
- 3: **for**  $i = 1$  To  $n$  **do** ▷ Train each expert
- 4:      $s_i \leftarrow D$
- 5:     **for**  $j = 1$  To  $t$  **do**
- 6:         Train  $f$  via  $D_i$
- 7:         Record correctness training subset:  $Correct = \{(G^r, G^p) \in D_i \mid L(f(G^r), G^p) = 0\}$
- 8:         Only select consistently predicted correctly samples:  $s_i \leftarrow s_i \cap \{Correct\}$
- 9:     **end for**
- 10:     Update:  $D_i \leftarrow D_i - s_i$
- 11:     Add expert  $f$  (as  $f_i$ ) and corresponding “correctness” training subset  $s_i$  to  $F$ :  $F \leftarrow F \cup \{(f, s_i)\}$
- 12: **end for**
- 13: Train chief expert  $f_{chief}$  via  $D$
- 14: Add expert  $f_{chief}$  to  $F$ :  $F \cup \{(f_{chief}, \emptyset)\}$
- 15: **return**  $F$

---

our code and trained checkpoints publicly upon acceptance of the paper.